

(p,d) and (p,t) Reactions on the Zn Isotopes at 17.5 MeV*

L. C. McINTYRE†

Palmer Physical Laboratory, Princeton University, Princeton, New Jersey

(Received 10 August 1966)

Angular distributions of the differential cross section for the (p,d) and (p,t) reactions on the five stable Zn isotopes, $Zn^{64,66,67,68,70}$, were obtained using 17.5-MeV protons. Between 9 and 15 deuteron groups were investigated for each isotope. Pickup of neutrons from the $1f_{5/2}$, $2p_{3/2}$, $2p_{1/2}$, and $1g_{9/2}$ subshells indicates considerable configuration mixing in the ground-state wave functions of the target nuclei. Several cases of “ J dependence” were observed. Distorted-wave Born approximation calculations were carried out and spectroscopic factors and occupation numbers are presented.

I. INTRODUCTION

THE (p,d) neutron pickup reaction is a useful tool for examining neutron-hole states and provides complementary information to the highly exploited (d,p) stripping reaction. In conjunction with the distorted-wave Born approximation (DWBA) theory of nuclear reactions, the (p,d) reaction can be used to determine the shell-model configurations present in the ground state of the target nucleus. The present work on the Zn isotopes is a continuation of previous similar studies on nuclei from Ca through Ni.¹⁻⁵

This previous work has shown that there is some configuration mixing in the $f_{7/2}$ shell; however, mixing in the $f_{5/2}-2p$ shell is considerably more pronounced. It is the purpose of this experiment to investigate how this configuration mixing continues in the Zn isotopes. The principal technique involves identification, for each deuteron group, of the subshell from which the picked-up neutron originated. The DWBA theory is then used to normalize the strengths of the transitions and occupation numbers for the various subshells in the target nucleus are calculated.

As is well known, the orbital angular-momentum transfer l_n can in many cases be determined by the shape of the angular distribution either empirically² or by comparison with DWBA calculations. In addition, it has recently been shown⁶⁻⁸ that it is possible to distinguish in some cases not only the l_n but the total angular-momentum transfer $j=l_n\pm\frac{1}{2}$. This “ J dependence” allows one to uniquely specify the subshell from which the neutron was picked up permitting assignment

of spin and parity to states reached in the (p,d) reaction from a 0^+ target nucleus.

In this experiment we have measured angular distributions of the differential cross section for the (p,d) reaction on the five stable zinc isotopes $Zn^{64,66,67,68,70}$ for an incident proton energy of 17.5 MeV. Angular distributions characteristic of $l_n=1$ and $l_n=3$ resulting from the pickup of neutrons from the $2p_{1/2}$, $2p_{3/2}$, and $1f_{5/2}$ subshells dominate the spectra. The $l_n=1$ angular distributions in several cases display “ J -dependent” features sufficient to distinguish $\frac{1}{2}^-$ from $\frac{3}{2}^-$ states. In all cases a relatively strong mixing of the $2p_{1/2}$ configuration in the ground state of the target nucleus was found. In addition, for the Zn^{68} and Zn^{70} targets the presence of a $1g_{9/2}$ configuration was noted. Three levels which could be postulated to be the result of $1f_{7/2}$ pickup were observed. DWBA calculations were carried out and spectroscopic factors extracted. Previous systematic studies of the zinc isotopes have been made by Lin and Cohen⁹ with the (d,p) reaction and by Zeidman *et al.*¹⁰ with the (d,t) reaction.

Tritons from the (p,t) reaction were recorded simultaneously with the deuterons and these results will also be presented. No analysis of the triton data was attempted.

II. EXPERIMENTAL METHOD

The 17.5-MeV proton beam from the Princeton fm cyclotron was used to bombard isotopically enriched Zn foils¹¹ of approximately 1 mg/cm² thickness. Stochastic extraction¹² of the beam was utilized to increase the beam duty cycle and thereby reduce pile-up. The reaction products were detected by a $\Delta E-E$ solid-state detector telescope mounted in a 20-in.-diam scattering chamber.¹³ Silicon surface-barrier detectors of 50- μ and 500- μ thickness were used for the ΔE and E counters, respectively. Particle identification was accomplished

* This work supported by the U. S. Atomic Energy Commission and the Higgins Scientific Trust Fund.

† Present address: Department of Physics, University of Arizona, Tucson, Arizona.

¹ E. Kashy, Phys. Rev. **134**, B378 (1964).

² E. Kashy and T. W. Conlon, Phys. Rev. **135**, B389 (1964).

³ T. W. Conlon, B. F. Bayman, and E. Kashy, Phys. Rev. **144**, 941 (1966).

⁴ R. Sherr, B. Bayman, E. Rost, M. E. Rickey, and C. G. Hoot, Phys. Rev. **139**, B1272 (1965).

⁵ R. Sherr, lectures presented at the Summer Institute for Theoretical Physics, Department of Physics and Astrophysics, University of Colorado, 1965 (to be published).

⁶ L. L. Lee, Jr., and J. P. Schiffer, Phys. Rev. **136**, B405 (1964).

⁷ R. Sherr, E. Rost, and M. E. Rickey, Phys. Rev. Letters **12**, 420 (1964).

⁸ C. Glasshausser, Ph.D. thesis, Princeton University, 1965 (unpublished).

⁹ E. K. Lin and B. L. Cohen, Phys. Rev. **132**, 2632 (1963).

¹⁰ B. Zeidman, J. L. Yntema, and B. J. Raz, Phys. Rev. **120**, 1723 (1960).

¹¹ The foils were obtained from Stable Isotopes Division, Oak Ridge National Laboratories, Oak Ridge, Tennessee. The purities are as follows: Zn^{64} -99.9%, Zn^{66} -98.8%, Zn^{67} -92.4%, Zn^{68} -98.5%, Zn^{70} -78.3%.

¹² H. O. Funsten, N. R. Roberson, A. Lieber, and R. Sherr, Rev. Sci. Instr. **35**, 1653 (1964).

¹³ A. Lieber, Nucl. Instr. Methods **26**, 51 (1964).

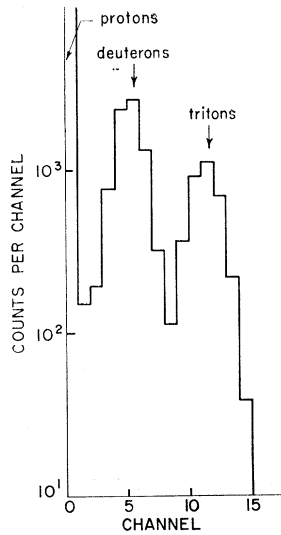


FIG. 1. Projection of a 16×256 -channel two-dimensional pulse-height spectrum on the 16-channel axis showing separation of protons, deuterons, and tritons.

by a pulse multiplier which formed the product $\Delta E \times E$ which is approximately proportional to MZ^2 of the incident particle. This pulse was applied to the 16-channel side of a 4096-channel two-dimensional pulse-height analyzer¹⁴ operated in the 16×256 -channel mode. The total energy signal E was applied to the 256-channel side. Protons, deuterons, and tritons were separated in this manner and two 256-channel energy spectra, one for deuterons and one for tritons, were extracted for each run, the protons being biased out. The projection of such a two-dimensional spectrum on the 16-channel axis, showing separation of protons, deuterons, and tritons, is shown in Fig. 1. This system is identical to that previously used in this laboratory.¹

After each run, the memory of the pulse-height analyzer was read out in the form of punched paper tape and Optikon photographs. The paper tape was

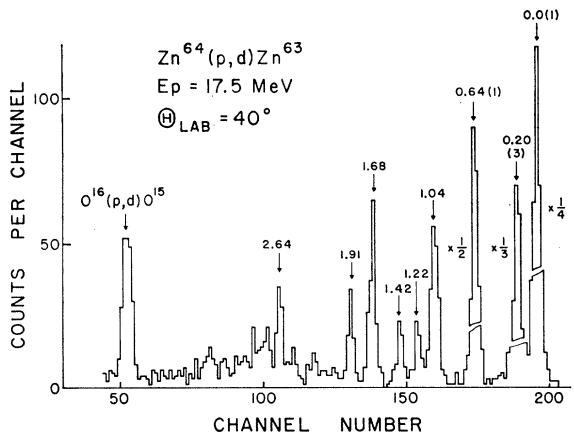


FIG. 2. Deuteron energy spectrum from the $Zn^{64}(p,d)Zn^{63}$ reaction at $\theta_{lab} = 40^\circ$. The numbers labeling the peaks are excitation energies in MeV. The numbers in parenthesis are values of l_n as determined from the shapes of the angular distributions.

¹⁴ Nuclear Data Model ND160.

subsequently used as input to an IBM 1620 computer which performed the necessary operations to produce the deuteron and triton spectra. The spectra were produced both on a line printer and on punched cards for later plotting by a Calcomp plotter.

Beam currents were typically 5–10 nA with a 10% duty cycle and 30-keV energy spread. Each angle required from 2–4 h running time. At the most forward angles a third detector was placed behind the E counter and was used to provide an anticoincidence signal to the analyzer, thus preventing proton pile-up pulses from being analyzed, resulting in somewhat cleaner spectra than otherwise. The over-all energy resolution was about 70 keV.

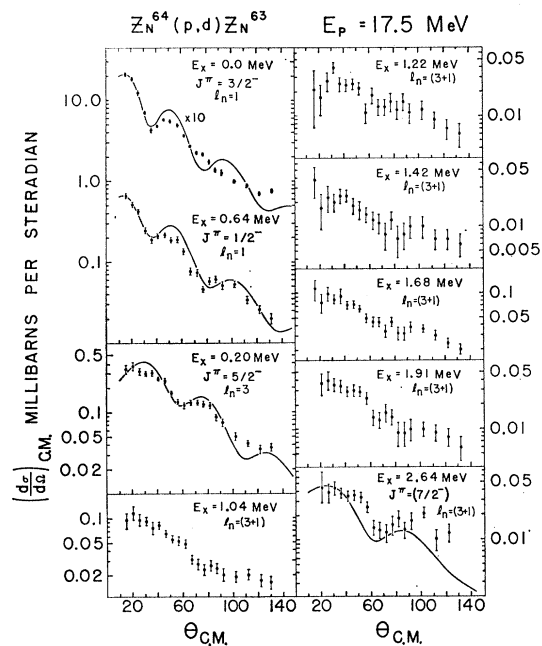


FIG. 3. Angular distributions of deuteron groups from the $Zn^{64}(p,d)Zn^{63}$ reaction. The solid curves are from DWBA calculations. The curve for the 2.64-MeV state was calculated with $l_n = 3, j = \frac{7}{2}$.

A monitor counter, which measured the elastically scattered protons at $\theta_{lab} = 90^\circ$, was used in order to normalize the cross sections within one angular distribution taken on different days. This was necessary because of the nonuniformity of target thickness. The beam current was also integrated and absolute cross sections determined for the strong states with an error of about $\pm 15\%$ estimated from the fluctuation of the monitor counter yield per integrated charge using different portions of the targets. This uncertainty in target thickness is the dominant source of error for the states with a relatively large cross section. In the case of cross sections less than about 0.1 mb/sr counting statistics become the major contributor to the uncertainty and they have correspondingly larger errors. The

TABLE I. Summary of results obtained from the (p,d) reaction on the Zn isotopes.

E_x (MeV)	$-Q$ (MeV)	l_n	J^π a	J^π b	$\left(\frac{d\sigma}{d\Omega}\right)_{c.m., \max}$ (mb/sr)	S	E_x (MeV)	$-Q$ (MeV)	l_n	J^π a	J^π b	$\left(\frac{d\sigma}{d\Omega}\right)_{c.m., \max}$ (mb/sr)	S
Zn⁶⁴(p,d)Zn⁶³							Zn⁶⁷(p,d)Zn⁶⁶						
0.00	9.63	1	$\frac{3}{2}^-$	$\frac{3}{2}^-$ c	2.1 (15°)	1.35	3.80	8.63	1			1.90 (15°)	0.8
0.20	9.83	3	$\sqrt{\quad}$	$\frac{1}{2}^- + \frac{5}{2}^-$ d	0.37 (20°)	2.8	4.00	8.83	1			0.25 (20°)	0.1
0.64	10.27	1	$\frac{1}{2}^-$	$\frac{1}{2}^-$ e	0.65 (15°)	0.84	4.10	8.93	1			0.77 (15°)	0.4
1.04	10.67	(3+1)	$(\frac{5}{2}^-)$		0.12 (20°)	0.7 ^f	4.30	9.13
1.22	10.85	(3+1)			0.04 (30°)	0.25 ^f	4.45	9.28
1.42	11.05	(3+1)			0.04 (15°)	0.25 ^f	5.00	9.83
1.68	11.31	(3+1)			0.12 (15°)	0.85 ^f							
1.91	11.54	(3+1)			0.04 (25°)	0.3 ^f							
2.64	12.27	(3+1)	$(\frac{7}{2}^-)$		0.04 (30°)	0.4 ^f							
Zn⁶⁶(p,d)Zn⁶⁵							Zn⁶⁸(p,d)Zn⁶⁷						
0.00	8.81	3	$\frac{5}{2}^-$	$\frac{5}{2}^-$ g	0.63 (35°)	4.1	0.00	7.98	3	$\frac{5}{2}^-$	$\frac{5}{2}^-$ g	0.82 (35°)	3.8
0.05	8.86	1	$\sqrt{\quad}$	$\frac{3}{2}^-$ g	0.73 (15°)	0.37	0.09	8.07	1	$\frac{3}{2}^-$	$\frac{3}{2}^-$ j	1.00 (20°)	0.40
0.11	8.92	1	$\sqrt{\quad}$	$\frac{3}{2}^-$ g	5.0 (15°)	2.2	0.18	8.16	1	$\frac{3}{2}^-$	$\frac{3}{2}^-$ i	0.51 (20°)	0.19
0.21	9.02	(1)	$\sqrt{\quad}$	$\frac{3}{2}^-$ g	0.32 (15°)	0.2	0.40	8.38	1	$\frac{3}{2}^-$	$\frac{3}{2}^-$ g	5.10 (15°)	1.76
0.88	9.69	1	$\frac{1}{2}^-$	$(\frac{1}{2}^-, \frac{3}{2}^-)$ g	0.64 (20°)	0.6	0.63	8.61	(4)	$\sqrt{\quad}$	$\frac{3}{2}^- + \frac{3}{2}^-$ g	0.18 (40°)	0.90
1.07	9.88	(3,4)		$\frac{3}{2}^- + \frac{3}{2}^-$ g	0.09 (35°)		0.87	8.85	(1)			0.07 (15°)	0.04
1.26	10.07	(3)			0.07 (30°)	0.7	1.00	8.98	(1)			0.11 (15°)	0.06
1.37	10.18	...			0.06 (30°)		1.18	9.16	1	$\frac{1}{2}^-$	$(\frac{1}{2}^-, \frac{3}{2}^-)$ g	0.29 (15°)	0.18
1.59	10.40	...			0.09 (25°)		1.59	9.57	...			0.03 (25°)	
1.96	10.77	(1)			0.09 (15°)	0.1	1.71	9.69	(3)			0.16 (35°)	1.3
2.22	11.03	(1)			0.09 (15°)	0.1	1.88	9.86	...			0.12 (20°)	
2.90	11.71	...	$(\frac{7}{2}^-)$		0.07 (15°)	1.2	2.16	10.14	...			0.09 (20°)	
							2.31	10.29	(1)			0.12 (20°)	0.1
							2.85	10.83	...			0.07 (20°)	
							3.85	11.83	(3)	$(\frac{7}{2}^-)$		0.04 (35°)	0.65
Zn⁶⁷(p,d)Zn⁶⁶							Zn⁷⁰(p,d)Zn⁶⁹						
0.00	4.83	3($\frac{5}{2}$) ^h	$\sqrt{\quad}$	0 ⁺	0.28 (30°)	0.44	0.00	6.97	1	$\frac{1}{2}^-$	$\frac{1}{2}^-$ g	3.78 (15°)	0.8
1.04	5.87	1($\frac{3}{2}$) ^h	$\sqrt{\quad}$	2 ⁺ i	0.81 (15°)	0.10	0.44	7.41	4	$\frac{1}{2}^-$	$\frac{1}{2}^- + \frac{3}{2}^-$ g	0.50 (40°)	1.6
1.87	6.70	1	$\sqrt{\quad}$	2 ⁺ i	0.06 (15°)	0.01	0.54	7.51	3	$\frac{1}{2}^-$	$\frac{3}{2}^-$ g	0.87 (35°)	3.5
2.44	7.27	(1)			0.07 (20°)	0.02	0.84	7.81	1	$\frac{1}{2}^-$	$\frac{3}{2}^-$ g	7.06 (15°)	1.9
2.77	7.60	1($\frac{3}{2}$) ^h			1.85 (20°)	0.52	1.18	8.15	...			0.24 (15°)	
2.95	7.78	3($\frac{3}{2}$) ^h			0.11 (35°)	0.47	1.61	8.58	1			0.64 (15°)	
3.10	7.93	1			0.31 (15°)	0.1	1.85	8.82	1			0.57 (15°)	0.27
3.22	8.05	1			0.45 (20°)	0.15	1.99	8.96	1			0.63 (15°)	0.33
3.35	8.18	1			0.39 (15°)	0.14	2.31	9.28	1			0.29 (15°)	0.18
3.51	8.34	1			0.87 (20°)	0.3	2.46	9.43	1			0.24 (15°)	0.16
3.68	8.51	1			0.68 (15°)	0.3	2.79	9.76	1			0.27 (20°)	0.21

^a Spin and parity as determined in this experiment. A $\sqrt{\quad}$ indicates that results are consistent with previous assignments but that spin and parity are not uniquely determined here.

^b Previous assignments.

^c J. B. Cumming and N. T. Porile, Phys. Rev. 122, 1267 (1961).

^d Reference 17.

^e Reference 10.

^f This is the $l_n=3$ spectroscopic factor. The $l_n=1$ portion is approximately a factor of 10 lower.

^g Reference 9.

^h The total angular-momentum transfer is given in parentheses following l_n .

ⁱ Reference 25.

^j Reference 26.

nominal target thicknesses were obtained by both weighing and by alpha-gauge measurements.¹⁵

Excitation energies of excited states are estimated to have an uncertainty of ± 30 keV.

III. RESULTS

Zn⁶⁴(p,d)Zn⁶³

The deuteron spectrum from the Zn⁶⁴(p,d)Zn⁶³ reaction at $\theta_{lab}=40^\circ$ is shown in Fig. 2. The angular distributions of the differential cross section for the various deuteron groups are shown in Fig. 3 along with the results of DWBA calculations to be discussed in Sec. IV. The error bars shown are due to counting statistics only. A summary of all observed levels, including excitation energy, Q value, l_n , and spin-parity assign-

¹⁵ J. A. Nolen, Jr., Ph.D. thesis, Princeton University, 1965 (unpublished).

ments is given in Table I. The Q values given in the second column are based on ground-state Q values taken from Ref. 16. Also presented in this table are maximum observed cross sections together with the angles at which they were observed. The last column gives spectroscopic factors to be discussed in Sec. IV.

The ground state of Zn⁶³ is known to have $J^\pi=\frac{3}{2}^-$ which is consistent with the observed $l_n=1$ angular distribution, indicating pickup of a $2p_{3/2}$ neutron. A recent experiment¹⁷ involving the γ rays following the Cu⁶³(p,n)Zn⁶³ reaction has proposed levels in Zn⁶³ at 0.190 and 0.246 MeV with spins $\frac{5}{2}^-$ and $\frac{1}{2}^-$, respectively. The angular distribution to the 0.20-MeV state seen here is predominantly $l_n=3$ and the excitation energy is in good agreement with 0.190 MeV. Both of these

¹⁶ J. H. E. Mattauch, W. Thiele, and A. H. Wapstra, Nucl. Phys. 67, 1 (1965).

¹⁷ L. Birstein, M. Harchol, A. A. Jaffe, and A. Tsukrovitz, Nucl. Phys. 84, 81 (1966).

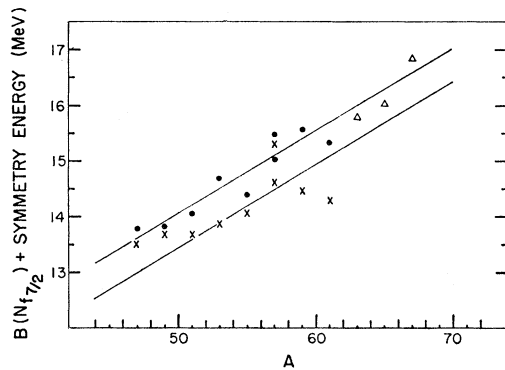


FIG. 4. Binding energy plus symmetry energy for an $f_{7/2}$ neutron as a function of A . The solid circles were calculated from the excitation energy of the center of gravity of known $f_{7/2}$ levels. The crosses were calculated for the lowest $f_{7/2}$ level in each case. The straight lines were drawn to reproduce the trend of the circles and crosses.

facts argue against significant contribution from the $\frac{1}{2}^-$, 0.246-MeV state. In addition, they¹⁷ report four closely spaced levels of undetermined spin and parity near 0.64-MeV excitation, whereas we observe what appears to be a single $\frac{1}{2}^-$ state.

By comparing the angular distribution of the $\frac{1}{2}^-$ state at 0.64 MeV to that of the $\frac{3}{2}^-$ ground state a “ J -dependent” feature is noted. The $\frac{1}{2}^-$ distribution has a minimum near 70° while the $\frac{3}{2}^-$ distribution has a slight shoulder at that angle. This feature has been previously observed.^{8,18} The angular distributions to the remaining rather weak levels are quite similar and can be fit by using roughly equal mixtures of $l_n=1$ and $l_n=3$ shapes. It can be conjectured that the state at 2.64 MeV corresponds to the pickup of a $1f_{7/2}$ neutron and is therefore tentatively assigned $\frac{7}{2}^-$. The binding energy of this neutron is in reasonable agreement with that expected for an $f_{7/2}$ neutron extrapolated from known $f_{7/2}$ levels.

The following procedure was used to estimate the expected excitation energy of states resulting from $f_{7/2}$ neutron pickup. The centers of gravity of known $f_{7/2}$ hole states¹⁹ in Ti, Cr, Fe, and Ni were taken from Table VII of Ref. 4. From these numbers values of the binding energy of an $f_{7/2}$ neutron were determined from the formula $B(N) = -Q + 2.225$ MeV. A symmetry

TABLE II. Predicted and observed excitation energies of $f_{7/2}$ hole states.

	E_x (predicted) (MeV)	E_x (observed) (MeV)
Zn ⁶³	2.86	2.64
Zn ⁶⁵	3.19	2.90
Zn ⁶⁶	6.39	...
Zn ⁶⁷	3.58	3.85
Zn ⁶⁹	4.15	...

¹⁸ C. A. Whitten, Jr., Ph.D. thesis, Princeton University, 1966 (unpublished).

¹⁹ Only the isospin $T_0 - \frac{1}{2}$ states were used since we do not expect to see any of the higher $T_0 + \frac{1}{2}$ states.

energy term,²⁰

$$\text{Symmetry energy} = [N - Z]/A \times 27 \text{ MeV},$$

was then added to $B(N)$ to remove the dependence of the binding energy on neutron excess. The resulting values of $B(N)$ + symmetry energy were plotted as a function of A . The results are presented in Fig. 4. The solid circles are values for the center of gravity of the $f_{7/2}$ levels; the crosses are results of the same calculation using the lowest observed $f_{7/2}$ state in each case. Straight lines were drawn to reproduce the trend of the points and serve in extrapolating to the region of the Zn isotopes. One might expect to observe an $f_{7/2}$ state in an extrapolated region somewhere between the two lines bracketing the lowest and center of gravity of known levels.

Using the upper extrapolated line, values of $B(N)$ + symmetry energy were taken and converted into excitation energies for the Zn isotopes. The results are given in Table II. The levels observed in this experiment, including the 2.64-MeV level in Zn⁶³, which are tentatively identified as resulting from $f_{7/2}$ pickup are also given in Table II and are shown as triangles on Fig. 4.

All the Zn⁶³ levels shown here have been previously reported except those at 1.91 and 2.64 MeV. The level at 1.68 is given as a doublet with energies 1.640–1.697 MeV by Anderson *et al.*²¹

Zn⁶⁶(p,d)Zn⁶⁵

The deuteron spectrum at $\theta_{\text{lab}} = 40^\circ$ and angular distributions are shown in Figs. 5 and 6. The four closely spaced levels near the ground state were not well resolved at all angles; however, sufficient separation was possible to unambiguously assign $l_n=3$ to the ground state and $l_n=1$ to the states at 0.05 and 0.11 MeV. The state at 0.21 MeV is most probably $l_n=1$, although this state has a previous assignment of $\frac{5}{2}^-$.⁹

The state at 0.88 MeV is assigned $\frac{1}{2}^-$ on the basis of the dip near 70° . The remaining weak states do not allow definite l_n assignments however probable values are given in Table I. The states at 1.07, 1.26, and 1.59 have been recently reported to be closely spaced doublets.²² The state at 2.90 MeV has about the right neutron binding energy to correspond to an $f_{7/2}$ pickup, and although the angular distribution is ambiguous, this state is tentatively assigned $\frac{7}{2}^-$. The predicted and observed values of excitation and binding energy for $\frac{7}{2}^-$ states are compared in Table II and Fig. 4. The levels at 2.22 and 2.90 MeV are previously unreported.

²⁰ F. G. Perey, Phys. Rev. **131**, 745 (1963).

²¹ J. D. Anderson, C. Wong, and J. McClure, Nucl. Phys. **36**, 161 (1962).

²² P. H. Stelson, Y. Cassagnou, F. Perey, J. McConnell, and M. Harlow, Bull. Am. Phys. Soc. **11**, 365 (1966).

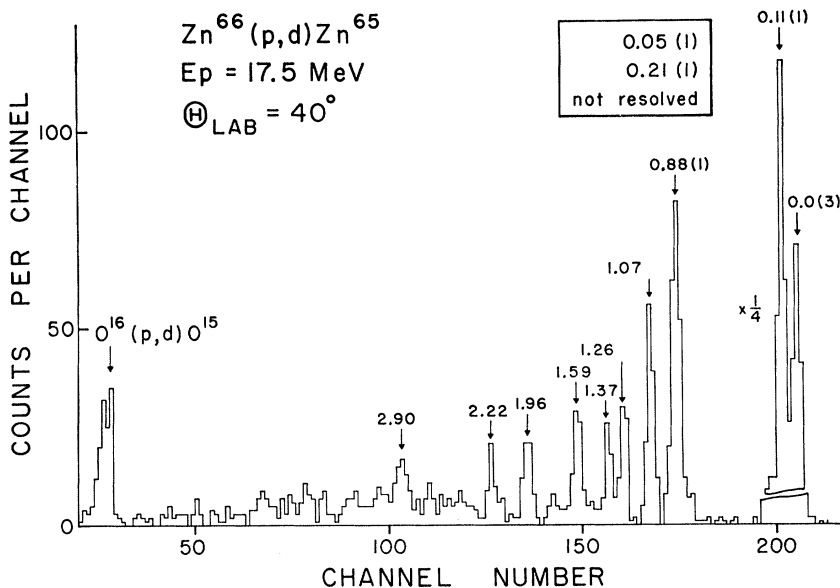


FIG. 5. Deuteron energy spectrum from the $Zn^{66}(p,d)Zn^{65}$ reaction at $\theta_{lab}=40^\circ$. The numbers labeling the peaks are excitation energies in MeV. The numbers in parentheses are values of l_n as determined from the shapes of the angular distributions.

$Zn^{67}(p,d)Zn^{66}$

This is the only odd- A target investigated and the deuteron spectrum at $\theta_{lab}=40^\circ$ and angular distributions are shown in Figs. 7, 8, and 9. This spectrum is dominated by $l_n=1$ transitions, the only $l_n=3$ being those to the ground and 2.95-MeV states.

The strong state at 2.77 MeV is believed to result from pickup of a $p_{3/2}$ neutron. A collective 3^- state has been observed in (d,d') ²³ and (α,α') ²⁴ at 2.81 MeV; however, it is unlikely that these are the same states, since a negative parity final state would most likely come from a d - or g -state neutron pickup and the magnitude and shape of the cross section observed argues against this possibility. An interesting feature of this reaction is the large fraction of strength in relatively highly excited states.

$Zn^{68}(p,d)Zn^{67}$

The deuteron spectra at $\theta_{lab}=35^\circ$ and angular distributions are given in Figs. 10–12. The $l_n=3$ angular distribution of the ground-state transition is consistent with the known $\frac{5}{2}^-$ spin of Zn^{67} . The states at 0.09 and 0.18 MeV previously reported²⁵ to have spins $\frac{5}{2}^-$ and $\frac{1}{2}^-$ have recently²⁶ been reassigned $\frac{1}{2}^-$ and $\frac{3}{2}^-$ on the basis of J dependence in the $Zn^{66}(d,p)Zn^{67}$ reaction. The angular distributions seen here confirm this reassignment. The 0.09-MeV level has a dip near 70° while the 0.18-MeV level has a shoulder at that angle.

²³ E. K. Lin, Nucl. Phys. **73**, 613 (1965).

²⁴ H. W. Broek, Phys. Rev. **130**, 1914 (1963).

²⁵ Nuclear Data Sheets, compiled by K. Way et al. (Printing and Publishing Office, National Academy of Sciences–National Research Council, Washington, D. C., 1963), NRC 59–1–9.

²⁶ J. P. Schiffer, D. von Ehrenstein, and L. L. Lee, Jr., Bull. Am. Phys. Soc. **11**, 100 (1966).

The strong state at 0.40 MeV and that at 0.63 MeV are consistent with previous $\frac{3}{2}^-$ and $\frac{5}{2}^+$ assignments, although the 0.63-MeV angular distribution is not unambiguously $l_n=4$. The state at 1.18 is assigned $\frac{1}{2}^-$ on the basis of the dip near 70° . The 3.85-MeV state has approximately the correct neutron binding energy to correspond to an $f_{7/2}$ pickup and since its angular distribution is not inconsistent with an $l_n=3$ shape it is tentatively assigned $\frac{7}{2}^-$. See Fig. 4 and Table II for predicted and observed excitation energies of this level.

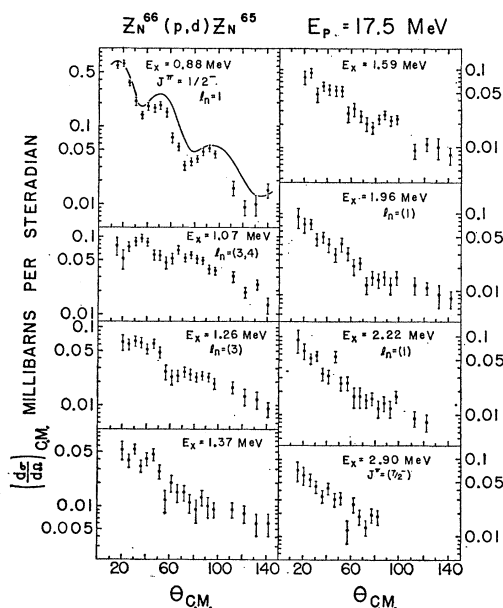


FIG. 6. Angular distribution of deuteron groups from the $Zn^{66}(p,d)Zn^{65}$ reaction. The solid curve is from a DWBA calculation.

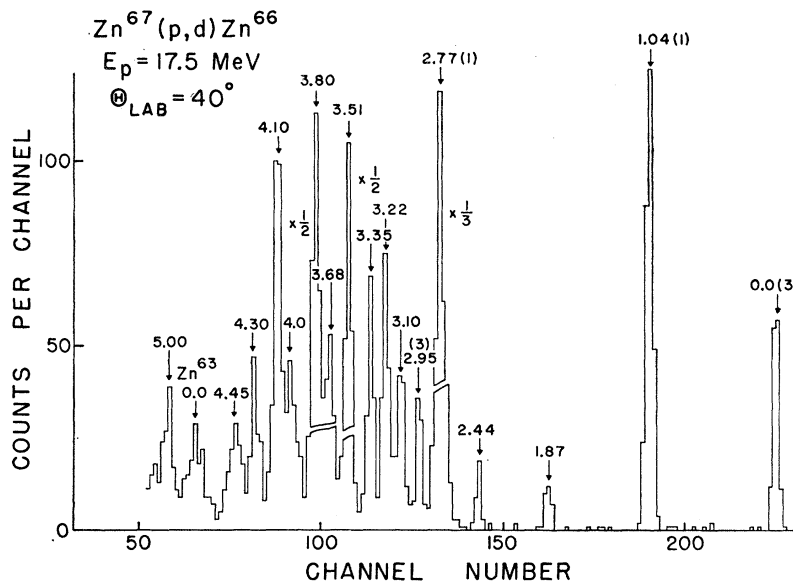


FIG. 7. Deuteron energy spectrum from the $Zn^{67}(p,d)Zn^{66}$ reaction at $\theta_{lab}=40^\circ$. The numbers labeling the peaks are excitation energies in MeV. The numbers in parentheses are values of l_n as determined from the shapes of the angular distributions.

The levels not previously reported are those at 1.88, 2.16, and 3.85 MeV.

$Zn^{70}(p,d)Zn^{69}$

The deuteron spectrum at $\theta_{lab}=40^\circ$ and angular distributions are shown in Figs. 13–15. The ground-state transition in this case corresponds to pickup of a $2p_{1/2}$ neutron. The angular distributions to the 0.44- and 0.54-MeV states are consistent with previous spin

assignments of $\frac{9}{2}^+$ and $\frac{5}{2}^-$ respectively. The very strong state at 0.84 MeV is assigned $\frac{3}{2}^-$ on the basis of the shoulder near 70° . A $d_{5/2}$ state is observed⁹ at approximately this excitation energy in the $Zn^{68}(d,p)Zn^{69}$ reaction.

The remaining states all display $l_n=1$ angular distributions; however, it is not possible to make definite J assignments. Impurity peaks from Zn^{64} and Zn^{68} are seen in this spectrum. Previously unreported levels are those at 1.18, 2.46, and 2.79 MeV.

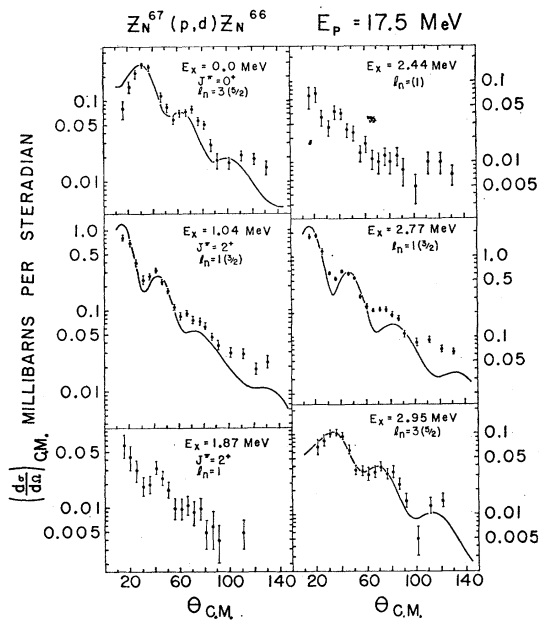


FIG. 8. Angular distribution of deuteron groups from the $Zn^{67}(p,d)Zn^{66}$ reaction. The solid curves are from DWBA calculations. The numbers in parentheses following the l_n values are the total angular-momentum transfer j .

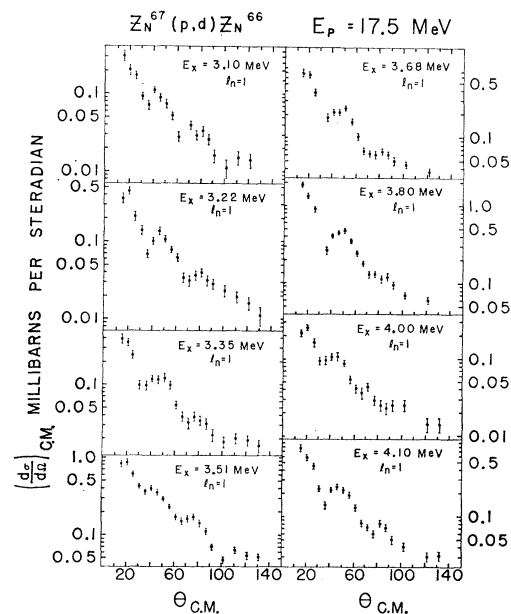
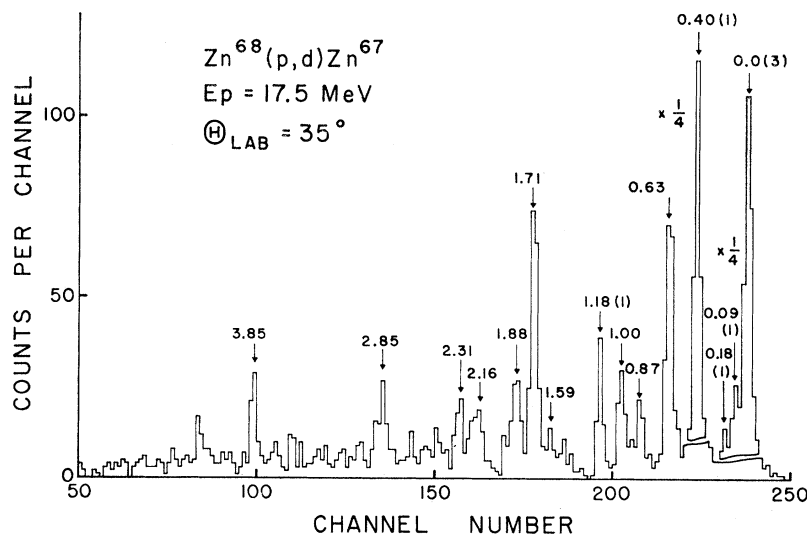


FIG. 9. Angular distributions of deuteron groups from the $Zn^{67}(p,d)Zn^{66}$ reaction.

FIG. 10. Deuteron energy spectrum from the $Zn^{68}(p, d)Zn^{67}$ reaction at $\theta_{lab} = 35^\circ$. The numbers labeling the peaks are excitation energies in MeV. The numbers in parentheses are values of l_n as determined from the shapes of the angular distributions.



The (p, t) Reactions

Spectra and angular distributions for the (p, t) reactions are given in Figs. 16 and 17. For the even- A targets Zn^{66} , Zn^{68} , and Zn^{70} , distinctive $l=0$ and $l=2$ angular distributions were observed for the transitions to the ground and first excited 2^+ state in the nuclide with two less neutrons. In Zn^{64} only the transition to the ground state of Zn^{62} was seen. The cross sections for these transitions increase with A as shown in Table III.

The Q values also vary with A such that the outgoing tritons, which are approximately at the Coulomb barrier energy for $Zn^{64}(p, t)Zn^{62}$, are progressively more ener-

getic as the target A increases. Thus a Coulomb barrier effect could account for this increase in cross section. Bassani, Hintz, and Kavaloski²⁷ have observed a decrease in the ground-state cross section in the target sequence Zn^{66} , Zn^{68} , Zn^{70} at 40 MeV.

The angular distributions for the 0.88-MeV $\frac{1}{2}^-$ state and the 1.26-MeV state in Zn^{65} were identified as $l=2$. The 1.65-MeV state in Zn^{68} has a $l=0$ angular distribution which constrains the spin of that state to 0^+ .

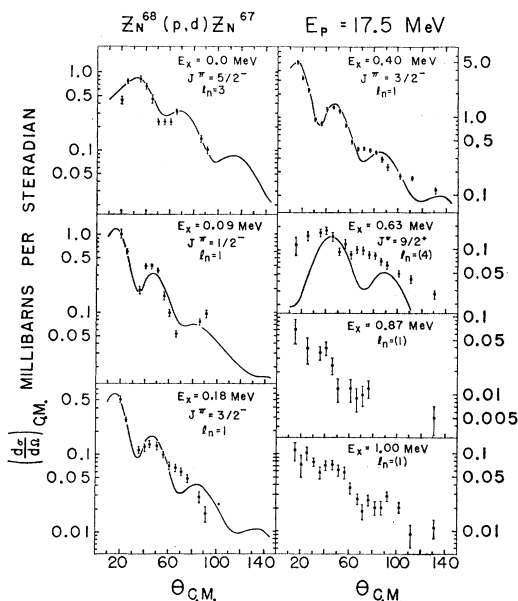


FIG. 11. Angular distributions of deuteron groups from the $Zn^{68}(p, d)Zn^{67}$ reaction. The solid curves are from the DWBA calculations.

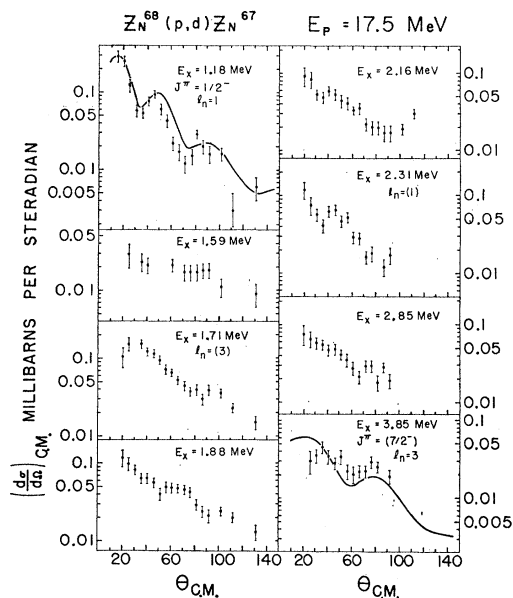


FIG. 12. Angular distributions of deuteron groups from the $Zn^{68}(p, d)Zn^{67}$ reaction. The solid curves are from DWBA calculations.

²⁷ G. Bassani, N. M. Hintz, and C. D. Kavaloski, Phys. Rev. **136**, B1006 (1964).

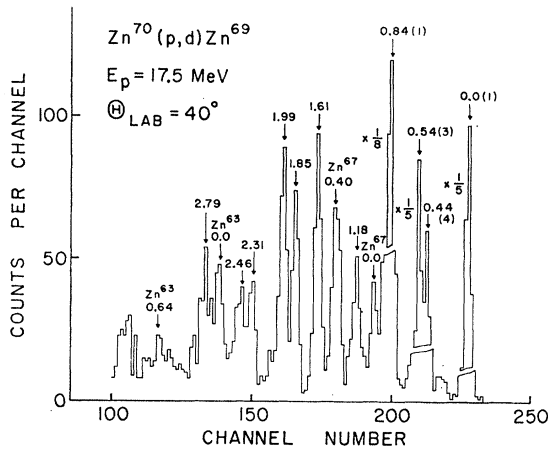


FIG. 13. Deuteron energy spectrum from the $Zn^{70}(p,d)Zn^{69}$ reaction at $\theta_{lab} = 40^\circ$. The numbers labeling the peaks are excitation energies in MeV. The numbers in parentheses are values of l_n as determined from the shapes of the angular distributions.

The 2.34-MeV level in Zn^{68} has a $l=2$ angular distribution.

The angular distributions to the remaining weak levels were ambiguous.

IV. DWBA ANALYSIS

The Oak Ridge DWBA code "JULIE"²⁸ was used to calculate theoretical angular distributions and extract

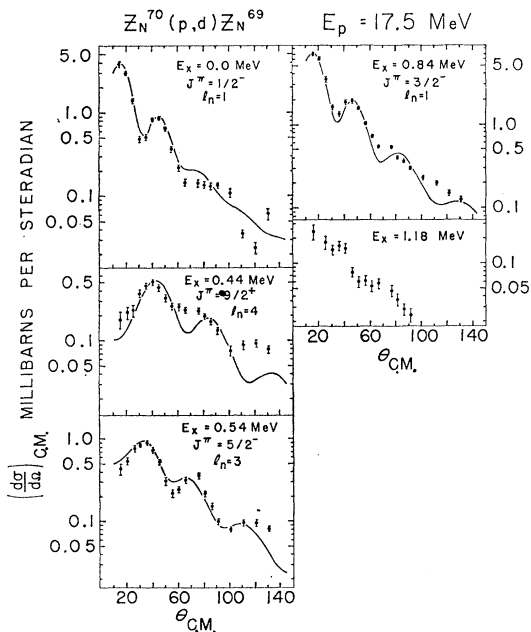


FIG. 14. Angular distributions of deuteron groups from the $Zn^{70}(p,d)Zn^{69}$ reaction. The solid curves are from DWBA calculations.

²⁸ R. H. Bassel, R. M. Drisko, and G. R. Satchler, Oak Ridge National Laboratory Report ORNL-3240, 1963 (unpublished).

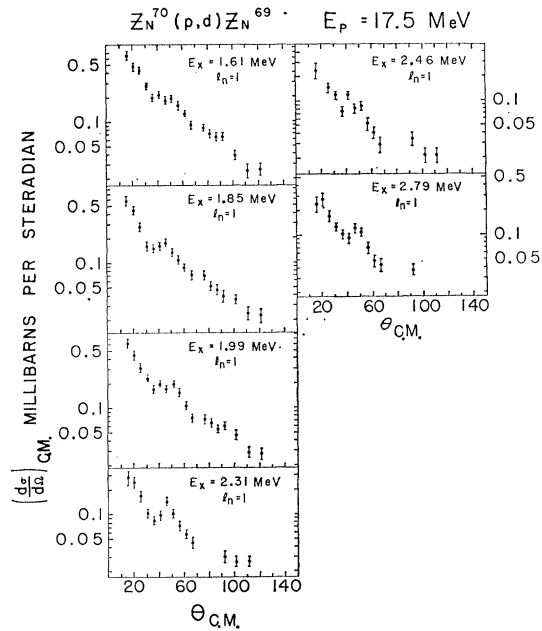


FIG. 15. Angular distributions of deuteron groups from the $Zn^{70}(p,d)Zn^{69}$ reaction.

spectroscopic factors. Optical-model parameters for the proton channel were taken from Perey,²⁰ and the deuteron parameters from Perey and Perey.²⁹ The "constant-geometry" proton parameters obtained from fitting elastic scattering at 17.0 MeV were chosen. The deuteron parameters are those obtained by using the set B geometrical parameters and elastic scattering data at 11.8 MeV. The parameters used are given in Table IV.

TABLE III. Q values and maximum $(d\sigma/d\Omega)_{c.m.}(\theta)$ for the (p,t) reactions.

Target	Zn^{64}	Zn^{66}	Zn^{67}	Zn^{68}	Zn^{70}
Q^a (MeV)	-12.54	-10.54	-9.61	-8.77	-7.22
$0^+ \rightarrow 0^+$ max cross section (mb/sr)	0.12	0.67	0.66	1.2	1.4
$0^+ \rightarrow 2^+$ max cross section (mb/sr)	...	0.13	...	0.24	0.47

^a From Ref. 16.

TABLE IV. Optical parameters.

	Proton channel	Deuteron channel
R_0 (F)	1.25	1.15
a (F)	0.65	0.81
R_0' (F)	1.25	1.34
a' (F)	0.47	0.68
V (MeV)	48.5	94.8
W_D (MeV)	12.4	22.5
V_{so} (MeV)	8.5	...

²⁹ C. M. Perey and F. G. Perey, Phys. Rev. 132, 755 (1963).

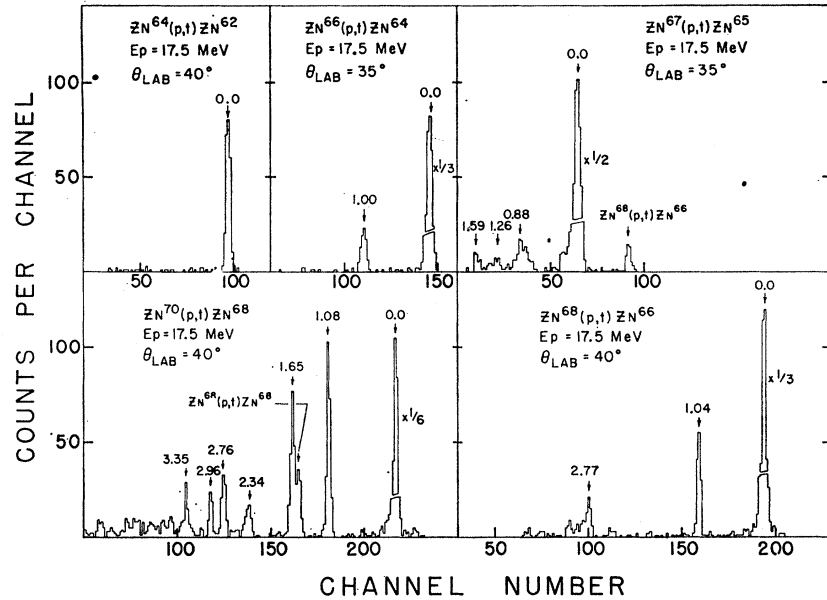


FIG. 16. Triton energy spectra from the (p,t) reaction on the Zn isotopes.

The form factors were calculated from a Woods-Saxon neutron well with parameters as follows: $R_0=1.25$ F, $a_0=0.65$, spin-orbit term $\lambda=35$ times the Thomas term. The depth was adjusted to bind the neutron with its separation energy. The simple zero-range, no cutoff version of the theory was used.

Results of these calculations are shown for some of the stronger transitions as the solid curves in Figs. 3, 6, 8, 11, 12, and 14. Reasonable agreement with the

experimental angular distributions were obtained in most cases, with $l_n=1$ and $l_n=3$ transitions being clearly distinguishable. As expected,⁸ the DWBA curves do not reproduce the observed "J dependence" distinguishing $\frac{1}{2}^-$ and $\frac{3}{2}^-$ states.

Spectroscopic factors were calculated from the formula

$$\left(\frac{d\sigma}{d\Omega}\right)_{\text{measured, max}} = S \left(\frac{d\sigma}{d\Omega}\right)_{\text{DWBA, max}}$$

For the weaker states, S was determined from a plot of maximum DWBA cross section versus Q value. Figure 18 shows this plot which was determined by points calculated for the stronger states where detailed compari-

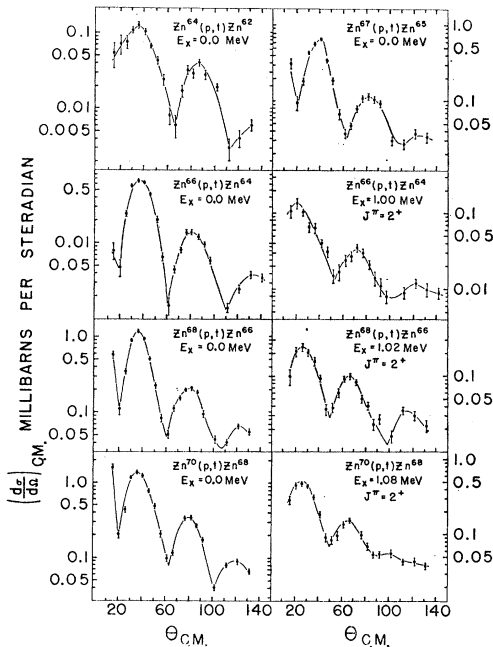


FIG. 17. Angular distributions of triton groups from the (p,t) reactions on the Zn isotopes. The curves were drawn through the points and have no theoretical significance.

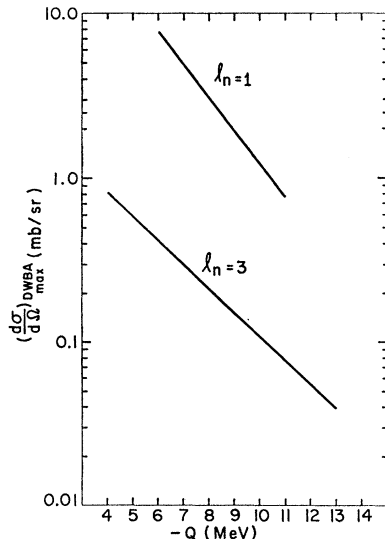


FIG. 18. Maximum (p,d) cross section from DWBA calculations as a function of Q value for $l_n=1$ and $l_n=3$.

TABLE V. Neutron occupation numbers.

	$2p_{3/2}$	$1f_{5/2}$	$2p_{1/2}$	$1g_{9/2}$	Addi- tional $l_n=1$	Addi- tional $l_n=3^a$	Total	$\sum S_<$
Zn ⁶⁴	1.4	2.8	0.8		0.2	2.4	7.6	5.6
Ni ⁶² b	1.7	3.6	0.7				6.0	6.0
Zn ⁶⁶	2.2	4.1	1.0		0.4	0.7	8.4	7.7
Zn ⁶⁷	0.6	0.9			2.3		3.8	8.75
Zn ⁶⁸	2.0	3.8	0.6	0.9	0.2	1.3	8.8	9.8
Zn ⁷⁰	1.9	3.5	0.8	1.6	1.5		9.3	11.8

^a The three states believed to result from $f_{7/2}$ pickup are not included in this table.

^b From Ref. 5.

son of shapes was of interest. In many $l_n=1$ cases where a J assignment could not be made, the spectroscopic factor was computed for the average of $J=\frac{1}{2}$ and $J=\frac{3}{2}$ values, which were in fact not very different. This average value is shown in Fig. 18. The $J=\frac{5}{2}$ and $J=\frac{7}{2}$ points taken together lie on the straight line labeled $l_n=3$. A summary of the results is given in Table I.

In addition, the sums of the spectroscopic factors of all transitions corresponding to pickup from a particular subshell were computed for the $2p_{3/2}$, $1f_{5/2}$, $2p_{1/2}$, and $1g_{9/2}$ subshells. These sums, according to the normalization used in the theory, should equal the number of neutrons in the corresponding subshell in the target nucleus and are called occupation numbers. In some cases, however, the total strength is split between states with isospin $T=T_0-\frac{1}{2}$ and $T=T_0+\frac{1}{2}$; T_0 being the isospin of the target. States with the larger T are known⁴ to lie at high excitation and are not expected to be observed here. This division of spectroscopic strength for pickup from a given subshell is given by Macfarlane and French³⁰ as

$$\sum_{T=T_0-1/2} S \equiv \sum S_< = \nu - \pi / (N - Z + 1),$$

where ν is the number of neutrons and π the number of protons in the subshell. The N and Z also refer to the target nucleus.

The total summed spectroscopic factor expected is $N-28$ if we ignore pickup in the $f_{7/2}$ shell and below. Since we only observe the $T=T_0-\frac{1}{2}$ states, however,

we should compare our totals with

$$\sum S_< = (N-28) - \pi / (N-Z+1),$$

where π is the number of protons above the $f_{7/2}$ shell, which in this case is two. These results are presented in Table V.

In the case of Zn⁶⁴, the total observed spectroscopic factor is 7.6, whereas $\sum S_<$ is only 5.6. This number was obtained assuming a mixture of $l_n=1$ and $l_n=3$ shapes with equal peak cross sections for the highest 6 levels in Zn⁶³ and, if this is justified, leads to the conclusion that considerable $1f_{7/2}$ strength is present in addition to that conjectured for the 2.64-MeV level. The occupation numbers obtained by Sherr⁵ for Ni⁶² are presented as a comparison since the neutron numbers for Ni⁶² and Zn⁶⁴ are the same. The latter numbers have been normalized to $N-28=6$ and are in reasonable agreement with the calculations of Auerbach.³¹

The Zn⁶⁶ total is 8.4 as compared with $\sum S_<=7.7$. The Zn⁶⁸ and Zn⁷⁰ totals are 8.8 and 9.3, respectively, as compared with $\sum S_<$ values of 9.8 and 11.8.

The Zn⁶⁷ case is special since A is odd. The ground-state spin of Zn⁶⁷ is $\frac{5}{2}^-$ and many of the states in Zn⁶⁶, e.g., those with $J^\pi=1^+, 2^+, 3^+$, or 4^+ , can be reached by either $l_n=1$ or $l_n=3$ pickup. Assuming the obviously dominant l_n value for each transition gives a summed spectroscopic factor of 3.8 whereas $\sum S_<=8.75$. The main deficiency is in the $l_n=3$ strength. This is probably due to the fact that a portion of the transitions assumed to be $l_n=1$ have a small $l_n=3$ component. Since $l_n=3$ transitions are inhibited by about a factor of 10 over those with $l_n=1$ by the centrifugal barrier a small mixture could contribute a sizeable spectroscopic factor.

In general the summed absolute spectroscopic factors from the DWBA theory seem to be in rough agreement with expected neutron numbers. Interesting points to be noted are the quite substantial $2p_{1/2}$ mixing in the Zn⁶⁴ and Zn⁶⁶ ground states and the large $1g_{9/2}$ component present in Zn⁶⁸ and Zn⁷⁰.

ACKNOWLEDGMENTS

The author would like to thank Professor R. Sherr for his interest in the discussions of this work. The assistance of W. Gerace with the various computer programs used is also gratefully acknowledged.

³⁰ J. B. French and M. H. Macfarlane, Nucl. Phys. **26**, 168 (1961).

³¹ N. Auerbach, Nucl. Phys. **76**, 321 (1966).